



**University of
Zurich**^{UZH}

**Zurich Open Repository and
Archive**

University of Zurich
University Library
Strickhofstrasse 39
CH-8057 Zurich
www.zora.uzh.ch

Year: 2024

Uromodulin processing in DNAJB11-kidney disease

Mariniello, Marta ; Schiano, Guglielmo ; Yoshifuji, Ayumi ; Gillion, Valentine ; Sayer, John Andrew ; Jouret, François ; Genkyst Study Group ; Le Meur, Yannick ; Cornec-Le Gall, Emilie ; Olinger, Eric Gregory ; Devuyst, Olivier

DOI: <https://doi.org/10.1016/j.kint.2023.11.008>

Posted at the Zurich Open Repository and Archive, University of Zurich

ZORA URL: <https://doi.org/10.5167/uzh-252242>

Journal Article

Accepted Version



The following work is licensed under a Creative Commons: Attribution-NonCommercial-NoDerivatives 4.0 International (CC BY-NC-ND 4.0) License.

Originally published at:

Mariniello, Marta; Schiano, Guglielmo; Yoshifuji, Ayumi; Gillion, Valentine; Sayer, John Andrew; Jouret, François; Genkyst Study Group; Le Meur, Yannick; Cornec-Le Gall, Emilie; Olinger, Eric Gregory; Devuyst, Olivier (2024). Uromodulin processing in DNAJB11-kidney disease. *Kidney International*, 105(2):376-380.

DOI: <https://doi.org/10.1016/j.kint.2023.11.008>

Uromodulin processing in *DNAJB11*-kidney disease

OPEN

Marta Mariniello^{1,9}, Guglielmo Schiano^{1,9}, Ayumi Yoshifuji^{1,9}, Valentine Gillion², John Andrew Sayer^{3,4}, François Jouret⁵, Genkyst Study Group, Yannick Le Meur⁶, Emilie Cornec-Le Gall⁷, Eric Gregory Olinger^{3,8} and Olivier Devuyst^{1,2}

¹*Mechanisms of Inherited Kidney Disorders, Institute of Physiology, University of Zurich, Zurich, Switzerland;* ²*Department of Nephrology, Cliniques Universitaires Saint-Luc, UCLouvain, Brussels, Belgium;* ³*Translational and Clinical Research Institute, Faculty of Medical Sciences, Newcastle University, Newcastle upon Tyne, UK;* ⁴*Renal Services, The Newcastle upon Tyne Hospitals NHS Foundation Trust, Freeman Road, Newcastle upon Tyne, UK;* ⁵*Division of Nephrology, University of Liège, Liège, Belgium;* ⁶*University of Brest, Unité Mixte de Recherche 1227, Centre Hospitalier Universitaire Brest, Brest, France;* ⁷*University of Brest, Inserm, Unité Mixte de Recherche 1078, Génétique, Génomique fonctionnelle et Biotechnologies, Centre Hospitalier Universitaire Brest, Brest, France;* and ⁸*Center for Human Genetics, Cliniques Universitaires Saint-Luc, UCLouvain, Brussels, Belgium*

Kidney International (2023) ■, ■-■; <https://doi.org/10.1016/j.kint.2023.11.008>

KEYWORDS: ADPKD; ADTKD; chaperone; secretory pathway; uromodulin

Copyright © 2023, International Society of Nephrology. Published by Elsevier Inc. This is an open access article under the CC BY-NC-ND license (<http://creativecommons.org/licenses/by-nc-nd/4.0/>).

Autosomal dominant polycystic kidney disease (ADPKD) and autosomal dominant tubulointerstitial kidney disease (ADTKD) are among the most frequent monogenic disorders causing chronic kidney disease. The main genes associated with ADPKD are *PKD1* and *PKD2*, encoding membrane and primary cilia proteins, polycystin-1 and polycystin-2, respectively, which are involved in multiple pathways regulating tubular cell differentiation. Recently, genes coding for proteins involved in the endoplasmic reticulum have been associated with rare, atypical forms of ADPKD. These genes include *ALG5*, *ALG8*, and *ALG9*, coding for enzymes involved in the lipid-linked oligosaccharide assembly for N-glycosylation of proteins; *GANAB*, coding for the α -subunit of the glucosidase II, which removes a glucose residue from immature glycoproteins before they enter the calnexin/calreticulin folding and quality control cycle; and *DNAJB11*, which encodes a cofactor of binding Ig protein (BiP), a chaperone required for the proper folding and assembly of secreted and membrane proteins (Figure 1a). The characterization of 77 affected individuals from 27 families carrying heterozygous *DNAJB11* variants revealed late-onset kidney failure, nonenlarged kidneys harboring small cysts and interstitial fibrosis, and gout, suggesting partial overlap between *DNAJB11*-associated ADPKD and ADTKD.^{1,2}

ADTKD is an increasingly recognized cause of kidney failure, characterized by tubular damage and interstitial fibrosis of the kidney in the absence of glomerular lesions. The most common gene associated with ADTKD is *UMOD*, coding for uromodulin—the most abundant protein excreted in normal urine. Uromodulin is a kidney-specific glycosylphosphatidylinositol-anchored glycoprotein that is essentially produced by the epithelial cells lining the thick ascending limb (TAL) of the loop of Henle. The protein contains 616 amino acids, including 48 cysteine residues engaged in 24 intramolecular disulfide bonds, as well as 8 N-glycosylation sites. After proper maturation and apical targeting in TAL cells, uromodulin is cleaved by a serine protease and assembled in the urine into polymers that form a gel-like

Correspondence: Olivier Devuyst, *Mechanisms of Inherited Kidney Disorders, Institute of Physiology, Winterthurerstrasse 190, Zurich, Switzerland CH-8057.*
E-mail: olivier.devuyst@uzh.ch; or olivier.devuyst@uclouvain.be

⁹MM, GS, and AY contributed equally to this report.

Received 17 April 2023; revised 4 October 2023; accepted 10 November 2023

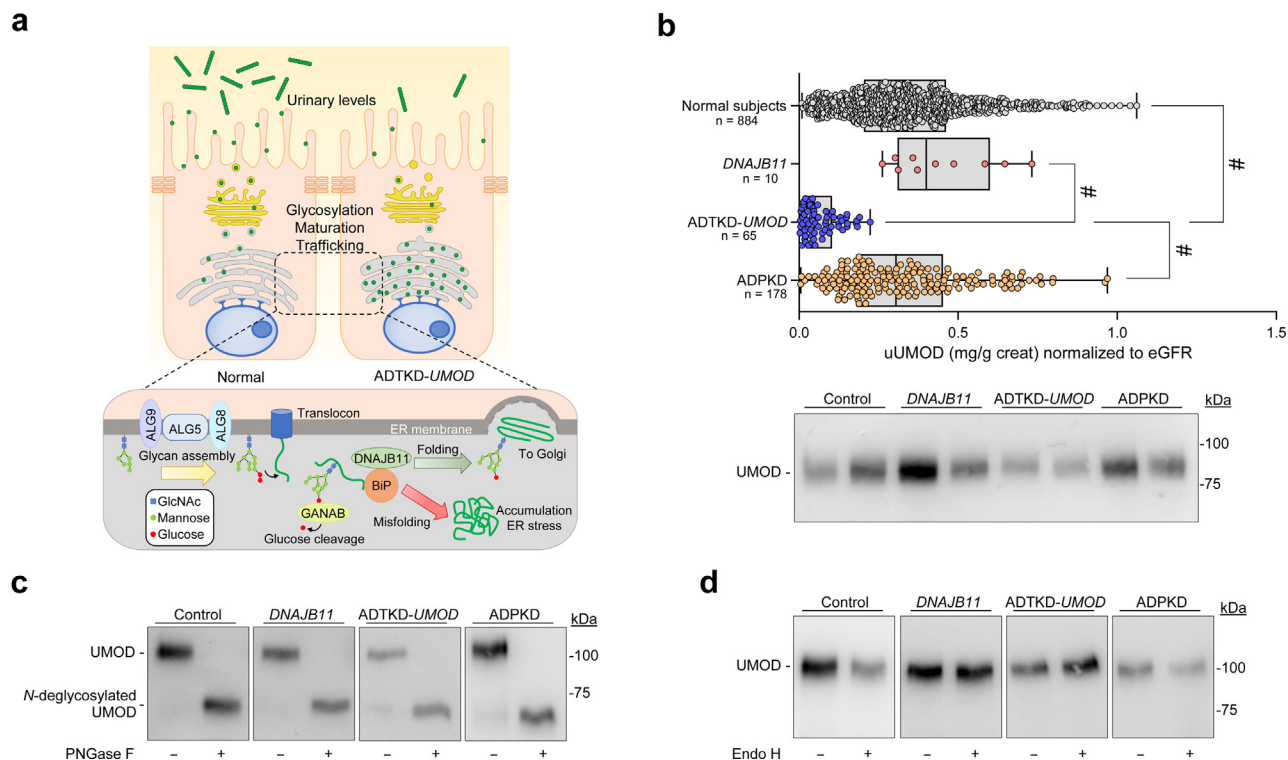


Figure 1 | Processing and urinary excretion of uromodulin (UMOD) in patients with *DNAJB11* mutations compared to normal subjects and patients with autosomal dominant tubulointerstitial kidney disease due to UMOD mutations (ADTKD-UMOD) or with autosomal dominant polycystic kidney disease (ADPKD). (a) Schematic diagram illustrating the maturation and trafficking of UMOD in normal and autosomal dominant tubulointerstitial kidney disease (ADTKD)–*UMOD* thick ascending limb cells. A detailed view of the endoplasmic reticulum (ER), including genes involved in atypical autosomal dominant polycystic kidney disease (ADPKD; *ALG5*, *ALG8*, *ALG9*, and *GANAB*), is shown on the bottom panel. (b) Urinary uromodulin (uUMOD) levels normalized to urinary creatinine and estimated glomerular filtration rate (Chronic Kidney Disease Epidemiology Collaboration) in patients with *DNAJB11* mutations compared with patients with ADTKD-*UMOD*, patients with ADPKD, and normal subjects. The uUMOD levels in *DNAJB11* samples are comparable to those of normal subjects and patients with ADPKD. Kruskal-Wallis test, followed by Tukey *post hoc* test: #*P* < 0.0001. The lower panel shows representative immunoblotting for UMOD in urine samples from corresponding patients and normal controls. Sample loading was normalized on urinary creatinine. Immunoblotting analysis was performed on *n* ≥ 3 independent patient samples per condition; 2 representative samples are shown. (c,d) Representative immunoblotting analyses of the effect of deglycosylation with (c) PNGase F (peptide-N-glycosidase F) and (d) Endo H (endoglycosidase H) on UMOD in urine samples from patients with mutations in *DNAJB11*, compared with patients with ADTKD-*UMOD*, patients with ADPKD, and normal subjects. No difference was observed in the glycosylation pattern. BiP, binding Ig protein; GalNAc, N-acetylglucosamine.

structure. The vast majority of disease-causing variants in *UMOD* causing ADTKD are heterozygous missense changes, often involving cysteine, that lead to the accumulation of uromodulin in the endoplasmic reticulum, damaging the TAL, inducing inflammation, and driving interstitial fibrosis (Figure 1a). ADTKD-*UMOD* is thus as a storage disease with a gain-of-toxic function, reflected by a sharp reduction of uromodulin excretion in the urine.³ Recently, intermediate-effect variants in *UMOD* have been associated with subtle

processing and maturation defects *in vitro* and intermediate urinary levels of uromodulin and milder kidney disease progression.⁴

The fact that *DNAJB11* (DnaJ homolog subfamily B member 11) and its partner BiP assist in the folding of client proteins in the endoplasmic reticulum⁵ led researchers to suggest that *DNAJB11*-related disease could include features of ADTKD-*UMOD* caused by defective processing of uromodulin. This hypothesis was supported by possible

Table 1 | Characteristics of patient cohorts and reference population

Group	N	Gender (M:F ratio)	Mean age, yr	uUMOD, mg/g creat	eGFR, ml/min per 1.73 m ²	uUMOD/eGFR, arbitrary units
<i>DNAJB11</i>	10	5:5	50 ± 20	33.5 ± 23.2	72 ± 37	0.45 ± 0.16
ADTKD- <i>UMOD</i>	65	26:39	38 ± 13	3.59 ± 3.63	46 ± 24	0.07 ± 0.05
ADPKD	178	95:83	54 ± 11	14.2 ± 9.7	44 ± 13	0.33 ± 0.2
Normal subjects	884	424:460	47 ± 17	34.1 ± 20.7	97 ± 18	0.35 ± 0.2

ADPKD, autosomal dominant polycystic kidney disease; ADTKD, autosomal dominant tubulointerstitial kidney disease; creat, creatinine; eGFR, estimated glomerular filtration rate (Chronic Kidney Disease Epidemiology Collaboration); F, female; M, male; uUMOD, urinary uromodulin. Data are expressed as mean ± SD unless otherwise indicated.

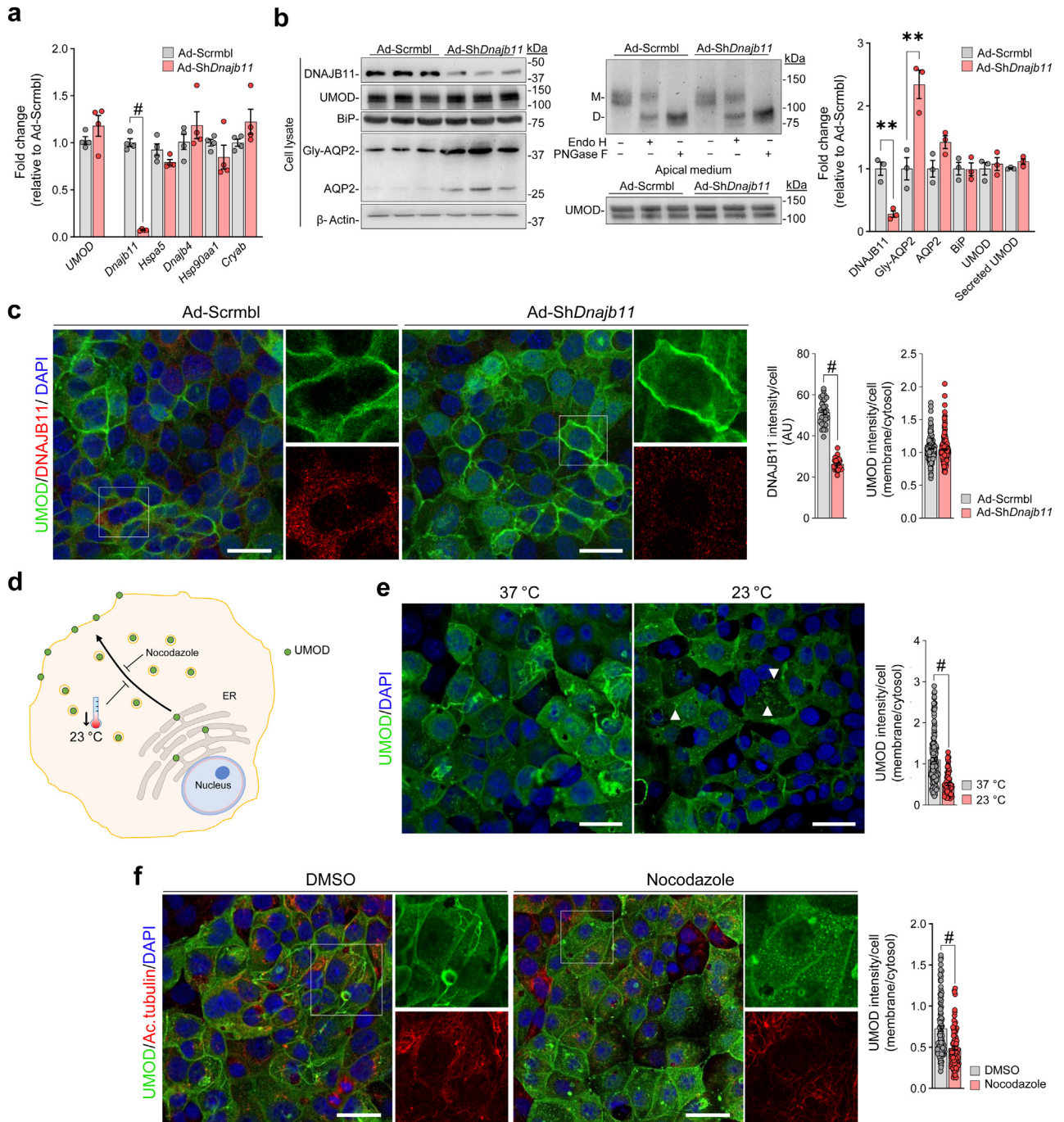


Figure 2 | Effect of *Dnajb11* silencing on uromodulin (UMOD) maturation and processing in mouse inner medullary collecting duct (mIMCD) cells. (a) Quantitative reverse transcriptase polymerase chain reaction analysis following *Dnajb11* knockdown ($n = 4$), showing $\approx 90\%$ transcript downregulation. Expression of *UMOD* and other chaperone genes was unaffected. Gene expression normalized on *Gapdh*. (b) Immunoblot analysis of DNAJB11, UMOD, binding Ig protein (BiP), and aquaporin-2 (AQP2) on mIMCD cells following 4 days of treatment with adenovirus expressing a short hairpin RNA against mouse *Dnajb11* (Ad-sh*Dnajb11*) or scramble adenovirus (Ad-Scrambl; left panel). Although UMOD and BiP levels were unchanged, a significant increase in glycosylated AQP2 levels was detected following *Dnajb11* knockdown. β -Actin was used as a loading control. UMOD glycosylation (top right panel) and secretion in culture medium (bottom right panel) were not impacted by *Dnajb11* knockdown. Densitometry analyses relative to Ad-Scrambl ($n = 3$). (c) Representative immunofluorescence staining for UMOD (green) and DNAJB11 (red) on mIMCD cells following treatment with Ad-sh*Dnajb11*, showing a strong reduction in signal intensity for DNAJB11. Neither intensity nor localization of the UMOD signal, analyzed as membrane/cytoplasmic ratio, is modified. (d) Schematic representation of UMOD trafficking and the effect of temperature shift and nocodazole treatment. (e) Immunofluorescence analysis of UMOD (green) in mIMCD cells following 1-hour incubation at 23 °C. The temperature shift induces translocation of UMOD into intracellular vesicular bodies (arrowheads), as indicated by the decreased membrane/cytosol ratio. (f) Immunofluorescence analysis of UMOD (green) and acetylated α -tubulin (Ac.Tubulin; red) in mIMCD cells following 1-hour treatment with 10 $\mu\text{g/ml}$ nocodazole. Disruption of microtubules impaired membrane trafficking of UMOD, as indicated by the decreased (continued)

intracellular accumulation of uromodulin in kidney biopsies from 2 *DNAJB11*-affected subjects.¹ However, such staining is operator dependent, requiring rigorous positive and negative controls. Furthermore, accumulation of uromodulin might depend on the underlying *UMOD* mutation, and the availability of kidney biopsies in ADTKD-*UMOD* is restricted. In that context, the urinary levels of uromodulin, normalized against residual estimated glomerular filtration rate values, are considered as a robust marker of its processing in TAL cells.^{4,6} Previous studies have demonstrated that modifications of the maturation and processing of uromodulin in the TAL cells are reflected by decreased urinary levels, which are proportional to the degree of protein maturation defect.^{4,6} Here, we measured the urinary levels of uromodulin in a cohort of patients harboring *DNAJB11* variants compared with healthy subjects and patients with ADTKD-*UMOD* or ADPKD and used well-established assays to assess the maturation and excretion of uromodulin in *DNAJB11*-deficient kidney cells.

RESULTS

Access to publicly available single-nucleus RNA-sequencing data of the human kidney showed that *DNAJB11* and *UMOD* are both highly expressed in the TAL cells, providing a basis for potential interactions (Supplementary Figure S1A and B).

We measured the levels of uromodulin in urine samples obtained from 10 individuals heterozygous for disease-causing variants in *DNAJB11* (Supplementary Figure S2), using a well-established enzyme-linked immunosorbent assay, compared with levels in patients with ADTKD-*UMOD* ($n = 65$) or ADPKD ($n = 178$) and a reference population (normal subjects, $n = 884$; Table 1). The range of urinary levels of uromodulin in subjects with *DNAJB11* mutations was similar to those in the reference population and the cohort with ADPKD, whereas dramatically lower values were detected in patients with ADTKD-*UMOD* (Figure 1b). Immunoblotting analyses confirmed the unchanged levels of uromodulin in urine, with no evidence for any change in glycosylation patterns, suggesting that only the mature protein is excreted in the urine of subjects with *DNAJB11* mutations (Figure 1c and d).

We next tested whether *Dnjab11* downregulation affects uromodulin processing in kidney tubular cells. To this end, we used mouse inner medullary collecting duct (mIMCD) cells stably expressing green fluorescent protein—tagged wild-type human uromodulin. We knocked down *Dnjab11* by treating the cells with an adenovirus expressing a short hairpin RNA against mouse *Dnjab11*, whereas a scramble adenovirus was used as control (Supplementary Figure S3A). No differences in transduction efficiency were observed after 4 days of silencing in scramble adenovirus- and adenovirus expressing a short hairpin RNA against mouse *Dnjab11*-treated cells, and no toxicity effect was detected compared

with untreated cells (Supplementary Figure S3B). Compared with scramble adenovirus-treated cells, short hairpin RNA treatment led to a sharp decrease of *Dnjab11* expression, whereas no significant changes were detected in the expression of *UMOD* and other chaperone genes coding for *DNAJB11* interaction partners (*Hspa5*, *Dnabj4*, *Hsp90aa1*, and *Cryab*; Figure 2a; Supplementary Figure S3C). Immunoblot analysis showed that *Dnjab11* silencing did not have any effect on uromodulin or on BiP levels, whereas it caused a sizable upregulation of the water channel aquaporin-2 (Figure 2b). Furthermore, *Dnjab11* silencing was not reflected by any difference in the glycosylation pattern of uromodulin or in its secretion in the apical medium (Figure 2b). These observations were confirmed by immunofluorescence analysis showing that trafficking of uromodulin to the plasma membrane was unaffected by *Dnjab11* downregulation in the mIMCD cells (Figure 2c). The stably transfected mIMCD cells represent a viable system to study uromodulin trafficking, as it can be modulated using physical and chemical agents (Figure 2d). Indeed, following either incubation at 23 °C or treatment with nocodazole, a well-established microtubule-disrupting agent,⁷ we observed a shift in uromodulin localization, from a predominantly plasma membrane-enriched signal to a more diffuse cytosolic vesicular pattern (Figure 2e and f). These results are in line with previous work showing that genetic disruption of the cytoskeletal network negatively impacts on uromodulin trafficking.⁸

DISCUSSION

The fact that the excretion and maturation of uromodulin are unchanged in patients with *DNAJB11* mutations contrasts with the strong decrease observed in patients with ADTKD-*UMOD*. Furthermore, the genetic downregulation of *Dnjab11*, to a level modeling haploinsufficiency, has no detectable impact on uromodulin maturation, trafficking, and secretion in the mIMCD cells. Because these cells are stably overexpressing uromodulin, one could expect that any effect of *DNAJB11* silencing on uromodulin processing would be particularly noticeable. These findings are in line with recent studies showing no change in uromodulin processing in *Dnjab11* knockout mice. Instead, the loss of *Dnjab11* was reflected by impaired cleavage of polycystin-1 and polycystin-1 dosage-dependent cystogenesis.⁹

Together, these data do not support that defective maturation or processing of uromodulin is involved in ADPKD caused by heterozygous *DNAJB11* mutations. Yet, considering the role of *DNAJB11* and BiP in the unfolded protein response (UPR),^{1,5} it is not excluded that variants in *DNAJB11* could affect the progression of ADTKD-*UMOD*. In such a scenario, loss-of-function *DNAJB11* mutations would negatively impact on the function of BiP, potentially worsening endoplasmic reticulum stress because of uromodulin

Figure 2 | (continued) membrane/cytosol ratio. High-magnification fields are shown as insets. Nuclei were counterstained with 4',6-diamidino-2-phenylindole (DAPI). Bar = 25 μm. Bars indicate mean ± SEM. Unpaired 2-tailed *t* test: ***P* < 0.01, #*P* < 0.0001. AU, arbitrary unit; D, deglycosylated; DMSO, dimethylsulfoxide; Endo H, endoglycosidase H; Gly, glycosylated; M, mature; PNGase F, peptide-N-glycosidase F. To optimize viewing of this image, please see the online version of this article at www.kidney-international.org.

aggregates and accelerating organ damage in ADTKD-*UMOD*. That *Dnajb11* silencing led to the upregulation of endogenous aquaporin-2 in mIMCD cells should also be noted, considering the role of the vasopressin V2R (vasopressin receptor 2)–cyclic adenosine monophosphate and aquaporin-2 pathway in ADPKD cystogenesis.¹⁰

DISCLOSURE

All the authors declared no competing interests.

DATA STATEMENT

All data are included in the article and/or supporting materials, including data (single-nucleus RNA sequencing for *UMOD* and *DNAJB11* in human kidney; *DNAJB11* mutation annotation; and interaction network of *DNAJB11*) derived from resources available in the public domain: Cellxgene repository (<https://cellxgene.cziscience.com/collections/b3e2c6e3-9b05-4da9-8f42-da38a664b45b>); and Ensembl canonical transcript for *DNAJB11* (ENST00000265028.8; <https://string-db.org>). Additional information can be provided on request to the principal investigators of the study.

ACKNOWLEDGMENTS

MM and OD are supported by the European Union's Horizon 2020 research and innovation program under the Marie Skłodowska-Curie grant (agreement no. 860977). OD is supported by the European Reference Network for Rare Kidney Diseases (project no. 739532), the Swiss National Science Foundation (grant 310030-189044), and the University Research Priority Program (URPP) ITINERARE at the University of Zurich. AY is supported by the Japan Society for the Promotion of Science Kagaku Kenkyuhi (JSPS KAKENHI) grant no. JP22K16378. EGO is supported by Postdoc Mobility-Stipend of the Swiss National Science Foundation grants (P2ZHP3_195181 and P500PB_206851), Kidney Research UK grant Paed_RP_001_20180925, and the Fonds National de la Recherche Luxembourg grant 6903109. JAS is supported by Kidney Research UK (Paed_RP_001_20180925 and RP_007_20210729) and the Northern Counties Kidney Research Fund (2019/01). The Genkyst Study Group is supported by a National Plan for Clinical Research (Programme Hospitalier de Recherche Clinique [PHRC] interregional GeneQuest, NCT02112136, EC-LG).

We thank Aleksandra Kokanovic and Nadine Nägele for expert technical assistance; Inès Dufour for clinical information on families with ADTKD; the German Chronic Kidney Disease study (Kai-Uwe Eckardt, Anna Köttgen, and Heike Meiselbach) for the reference population with ADPKD; and all participating patients and families.

SUPPLEMENTARY MATERIAL

[Supplementary File \(Word\)](#)

Supplementary Figure S1. Single-nucleus RNA sequencing of human kidney. (A,B) Feature plot (left) and dot plot (right) of (A) *DNAJB11* and (B) *UMOD* in a single-nucleus RNA-sequencing dataset of human kidney. *DNAJB11* shows strong expression in *CLDN16*-positive thick ascending limbs (TALs; TAL2) and type B intercalated (ICB) and type A intercalated (ICA) cells, whereas *UMOD* is almost exclusively expressed in the TAL clusters. ATL, ascending thin limb; DCT,

distal convoluted tubule; ENDO, endothelial cell; FIB, fibroblast; LEUK, leukocyte; MES, mesangial cell; PC, principal cell; PEC, parietal epithelial cell; PODO, podocyte; PT, proximal tubule; PTVCAM1, vascular cell adhesion molecule 1–positive proximal tubule.

Supplementary Figure S2. Clinical, genetic, and biochemical characteristics of patients with *DNAJB11* mutations. Top panel: domain architecture of *DNAJB11*. Mutations found in the *DNAJB11* patients are indicated. Bottom panel: clinical and biological features of patients with *DNAJB11* mutations. The annotation was performed on the Ensembl canonical transcript for *DNAJB11* (ENST00000265028.8). Cys-rich, cysteine-rich domain; Dim, dimerization domain; G/F, glycine/phenylalanine-rich domain; la/b, bipartite substrate-binding domain; SS, signal sequence.

Supplementary Figure S3. *Dnajb11* silencing protocol and interaction network. (A) Schematic diagram illustrating the transduction protocol in mouse inner collecting duct (mIMCD) cells expressing wild-type uromodulin coupled to the green fluorescent protein (UMOD-GFP). (B) Transduction efficiency (left) and cell viability assessed by MTT cytotoxicity assay (right) in adenovirus expressing a short hairpin RNA against mouse *Dnajb11* (Ad-sh*Dnajb11*) or scramble adenovirus (Ad-Scrambl) following 4 days of treatment, showing comparable transduction efficiency and mortality. (C) Interaction network of *DNAJB11* and related molecular chaperones. Data obtained from STRING (<https://string-db.org/> accessed on 16.12.2022).

Supplementary Table S1. Primers used for quantitative reverse transcriptase polymerase chain reaction (RT-qPCR).

Supplementary Methods.

Supplementary References.

REFERENCES

- Cornec-Le Gall E, Olson RJ, Besse W, et al. Monoallelic mutations to *DNAJB11* cause atypical autosomal-dominant polycystic kidney disease. *Am J Hum Genet.* 2018;102:832–844.
- Huynh VT, Audrézet MP, Sayer JA, et al. Clinical spectrum, prognosis and estimated prevalence of *DNAJB11*-kidney disease. *Kidney Int.* 2020;98:476–487.
- Devuyt O, Olinger E, Weber S, et al. Autosomal dominant tubulointerstitial kidney disease. *Nat Rev Dis Primer.* 2019;5:60.
- Olinger E, Schaeffer C, Kidd K, et al. An intermediate-effect size variant in *UMOD* confers risk for chronic kidney disease. *Proc Natl Acad Sci U S A.* 2022;119:e2114734119.
- Shen Y, Hendershot LM. ERdj3, a stress-inducible endoplasmic reticulum DnaJ homologue, serves as a cofactor for BiP's interactions with unfolded substrates. *Mol Biol Cell.* 2005;16:40–50.
- Olinger E, Hofmann P, Kidd K, et al. Clinical and genetic spectra of autosomal dominant tubulointerstitial kidney disease due to mutations in *UMOD* and *MUC1*. *Kidney Int.* 2020;98:717–731.
- Vasquez RJ, Howell B, Yvon AM, et al. Nanomolar concentrations of nocodazole alter microtubule dynamic instability *in vivo* and *in vitro*. *Mol Biol Cell.* 1997;8:973–985.
- Joseph CB, Mariniello M, Yoshifuji A, et al. Meta-GWAS reveals novel genetic variants associated with urinary excretion of uromodulin. *J Am Soc Nephrol.* 2022;33:511–529.
- Ghosh RS, Zhigui L, Guo Z, et al. *Dnajb11*-kidney disease develops from reduced polycystin-1 dosage but not unfolded protein response in mice. *J Am Soc Nephrol.* 2023;34:1521–1534.
- Devuyt O, Torres VE. Osmoregulation, vasopressin, and cAMP signaling in autosomal dominant polycystic kidney disease. *Curr Opin Nephrol Hypertens.* 2013;22:459–470.